IOP Conf. Series: Materials Science and Engineering **256** (2017) 012027 doi:10.1088/1757-899X/256/1/012027

# The phase-field modeling of the self-organized phase growth with three-fold symmetry

**A R Akhmatkhanov*, A I Lobov, M A Chuvakova, E D Saveliev and V Ya Shur**

School of Natural Sciences and Mathematics, Ural Federal University,
620000 Ekaterinburg, Russia

*andrey.akhmatkhanov@urfu.ru

**Abstract.** The formation of self-organized domain patterns during polarization reversal in highly non-equilibrium switching conditions was studied by us earlier in the single crystals of lithium niobate and lithium tantalate. In this paper, we used the phase-field simulation to verify the analogy between self-organized growth of domains and new phase during the first order phase transition. The crystal symmetry $C_{3v}$ was taken into account. The similarity of simulated and experimentally observed shapes of isolated domains was achieved.

## 1. Introduction

The phase-field model is widely used as a powerful computational method for modeling and predicting morphological and microstructure evolution in materials [1]. It has been shown that the model can be used successfully for studying of the formation of self-assembled structures during the first order phase transitions in highly non-equilibrium conditions, for example for description of dendritic crystal growth [2, 3]. The formation of self-assembled structures including the dendrite ones was demonstrated experimentally [4-8] and the phase diagram of the most common structure types was predicted [2,9,10]. However, the first order phase transitions including the crystallization from the melt possess the limited range of control parameters thus prohibiting the realization of all predicted types of structure in one system. This fact stimulates searching new systems with simple variation of control parameters. It is known that the evolution of ferroelectric domains during polarization reversal can be considered as an analog of the first-order phase transformation with electric field as a driving force [11-14]. The highly non-equilibrium switching conditions can be realized in ferroelectrics in wide range of control parameters. The complementary methods of domain visualization with high spatial and temporal resolutions are available [15-17]. The growth of self-organized dendrite domain patterns in ferroelectric lithium niobate ($LiNbO_3$, LN) and lithium tantalate single crystals with $C_{3v}$ symmetry was demonstrated by us earlier [4-8, 18]. Their great practical importance enabled the growth of the large crystals with extremely high uniformity. It was shown that the formed structures could demonstrate the $C_3$ and the $C_6$ envelope symmetry depending on the growth conditions [4-8, 18].

In this paper, we present the results of application of phase-field model to the domain growth to verify the analogy between self-organized growth of domains and new phase during the first order phase transition. The $C_{3v}$ symmetry of the crystals was taken into account.

## 2. Experimental results

Two self-organized domain patterns appeared during polarization reversal in LN single crystals have been analyzed.

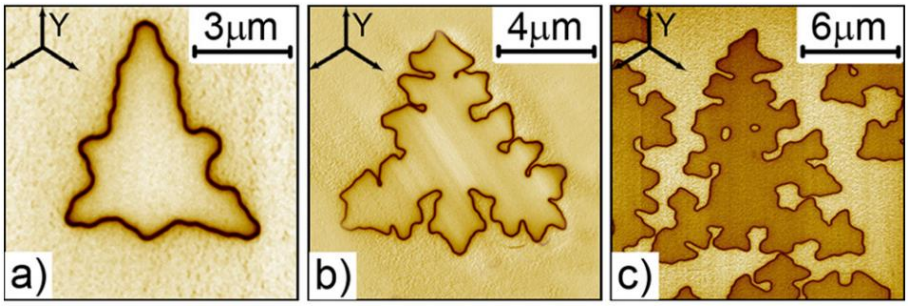


**Figure 1.** Piezoelectric force microscopy (PFM) image of dendrite structures obtained in stoichiometric LN at $230^0$C for various numbers of rectangular field pulses: (a) single pulse $E_{max}$=1.6 kV/mm, (b) two pulses $E_{max}$=1.6 kV/mm, (c) three pulses $E_{max}$=1.5 kV/mm. Reprinted with permission from [5]. Copyright 2012, AIP Publishing LLC.

The first object was the dendrite domains appeared in stoichiometric LN crystals at the temperatures above 230°C (Fig. 1) [5]. After partial switching from single domain state, the dendrite domains with sizes ranging from 3 to 30 μm were distributed over the Z polar surface covered by the electrode. The domain shape was close to six-ray stars with rays along crystallographic Y axes (Fig. 1). Y+ oriented rays were essentially longer than Y- ones. Several field pulses led to formation of more complicated dendrite structures (Fig. 1b,c).The second object was the domains growing in LN with surface layer modified by proton exchange (PE). They formed the self-organized sub-micron scale dendrite domain patterns consisting of the stripes oriented along the X crystallographic directions separated by the arrays of dashed residual domains (Fig. 2) [18]. The domain stripes formed as a result of branching of three Y oriented rays. The branching period was about 2 μm, close to the thickness of the PE layer. This process led to formation of the self-organized stripe structure with period of the dashed structure from 2 to 3 μm.

The obtained results demonstrate that the envelopes of self-organized domain structures in LN can follow both the crystal cymmetry $C_3$ (Fig. 1) and the higher symmetry $C_6$ (Fig. 2).

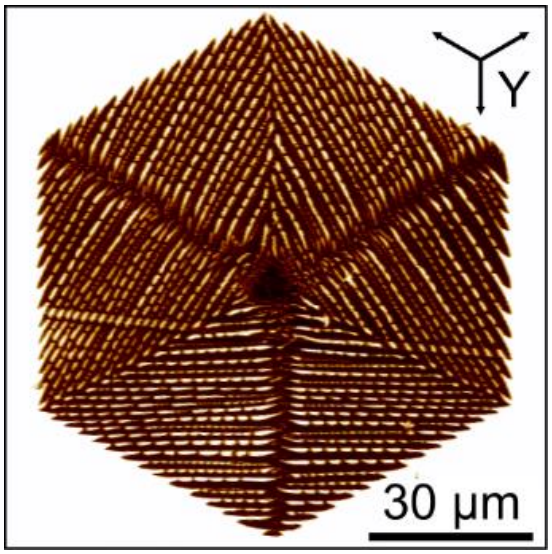


**Figure 2.** The self-organized domain structure obtained at the Z+ surface of LN with Z- surface modified by PE. PFM, phase signal. Dark area corresponds to the switched domains. Reprinted with permission from [18]. Copyright 2017, AIP Publishing LLC.

## 3. Phase-field modeling

The formation of the self-organized domain patterns was analyzed within the phase-field model for one component crystallization from the melt based on the analogy between the sideways motion of domain walls and the phase boundary motion during the first order phase transformations [19]. In this case, the main factor limiting the phase boundary motion velocity was the local temperature increase due to release of crystallization latent heat.

We have used the exothermal model of the first order phase transformation based on the time-dependent Ginzburg-Landau equation and the heat conductivity equation [2]. The model included two variables: the phase-field $p(r,t)$ and the temperature $T(\mathbf{r},t)$. The value $p(\mathbf{r},t)=0$ corresponds to the liquid phase and the $p(\mathbf{r},t)=1$ – to the solid phase. The phase boundary corresponds to a narrow layer, where $p(\mathbf{r},t)$ values lie between 0 and 1.

The following expression of Ginzburg-Landau free energy have been used:

$$\Phi(p,m) = \int (½\ \varepsilon^2 |\nabla p|^2 + F(p,m))\mathrm{d}\mathbf{r} \quad (1)$$

where $\varepsilon$ is a small parameter determining the width of phase boundary, $m$ is parameter determining the oversaturation, $F$ is two-well potential with local minima at $p = 0$ and $p = 1$ for any $m$. For the phase-field models of such type, the $F$ function is usually chosen as [2]:

$$F(p,m) = ¼\ p^4 – (½ - m/3)p^3+(¼ - ½\ m)\ p^2 \quad (2)$$

Based on the kinetic equation $\tau\partial p/\partial t = -\delta\Phi/\delta p$, we will get for the 2D problem taking into account that ε parameter is a function of angle between the normal to phase boundary and certain predefined direction ($\varepsilon=\varepsilon(\theta)$):

$$\tau\frac{\partial p}{\partial t} = -\frac{\partial}{\partial x}\left(\varepsilon\varepsilon'\frac{\partial p}{\partial y}\right) + \frac{\partial}{\partial y}\left(\varepsilon\varepsilon'\frac{\partial p}{\partial x}\right) + \nabla(\varepsilon^2\nabla p) + p(1-p)(p-\frac{1}{2}+m) \quad (3)$$

where $\tau$ is a small positive constant and the prime means the derivative $\mathrm{d}/\mathrm{d}\theta$. According to the obtained experimental results, the anisotropy of the parameter $\varepsilon(\theta)$ was chosen as a sum of $C_3$ and $C_6$ symmetry terms:

$$\varepsilon(\theta) = \varepsilon_0\ (1+\delta(\beta\cos(3\theta)+(1-\beta)\cos(6\theta))) \quad (4)$$

where $\varepsilon_0$ is an average value of interface energy, $\delta$ is anisotropy value, and $\beta$ is a relative input of $C_3$ symmetry term.

The following formula was used for temperature dependence of oversaturation:

$$m(T) = (\alpha/\pi)\ \arctan(\gamma(T_e-T)) \quad (5)$$

where $\alpha$ and $\gamma$ are the positive constants ($\alpha<1$), $T_e$ is an equilibrium temperature, $T$ is a local temperature.

The temperature in each point was calculated using the heat conductivity equation at the boundary with additional heat source:

$$\frac{\partial T}{\partial t} = \nabla^2 T + K\frac{\partial p}{\partial t} \quad (6)$$

where $K$ is normalized latent heat of crystallization.

The computer modeling consisted in the solving of the system of differential equations (3) and (6). For the initial moment, the phase-field $p(\mathbf{r},0)$ corresponded to one small circular region of solid phase in the center and the temperature in the whole volume was equal to $T_e$.

We have studied also the influence of noise on the obtained structure parameters. The additional term $ap(1-p)\chi$, where $a$ is noise amplitude, $\chi$ – random number uniformly distributed in the range [-½;½], was added to the equation (3).

The parameter values, used for the computer modeling are presented in Table 1.

The obtained self-organized structures are presented in Figure 3. It is clearly seen that the increase of relative input of $C_3$ term leads to transition from the hexagonal envelope shape to the triangular one.

We have analyzed the obtained transition in terms of change of the envelope shape constant $C$ (Fig. 4) calculated as:

$$C = S/R^2 \tag{7}$$

where $S$ is the area of obtained envelope, $R$ is the envelope radius corresponding to the maximum distance between the center of the structure and its point at the border.

**Table 1.** The values of the parameters used for the computer simulation.

| Parameter | Value |
|---|---|
| Anisotropy terms | $C_3$ and $C_6$ |
| Input of $C_3$ symmetry ($\beta$) | from 0 to 1 |
| Latent heat ($K$) | 1.5 |
| Equilibrium temperature ($T_{eq}$) | 0.9 |
| Noise amplitude ($a$) | 0.01 |
| Average interface energy ($\varepsilon_0$) | 0.1 |
| Anisotropy value ($\delta$) | 0.2 |
| The constants for calculating the oversaturation ($\alpha$ and $\gamma$) | 0.9 and 10 |
| $\tau$ parameter | 0.0003 |

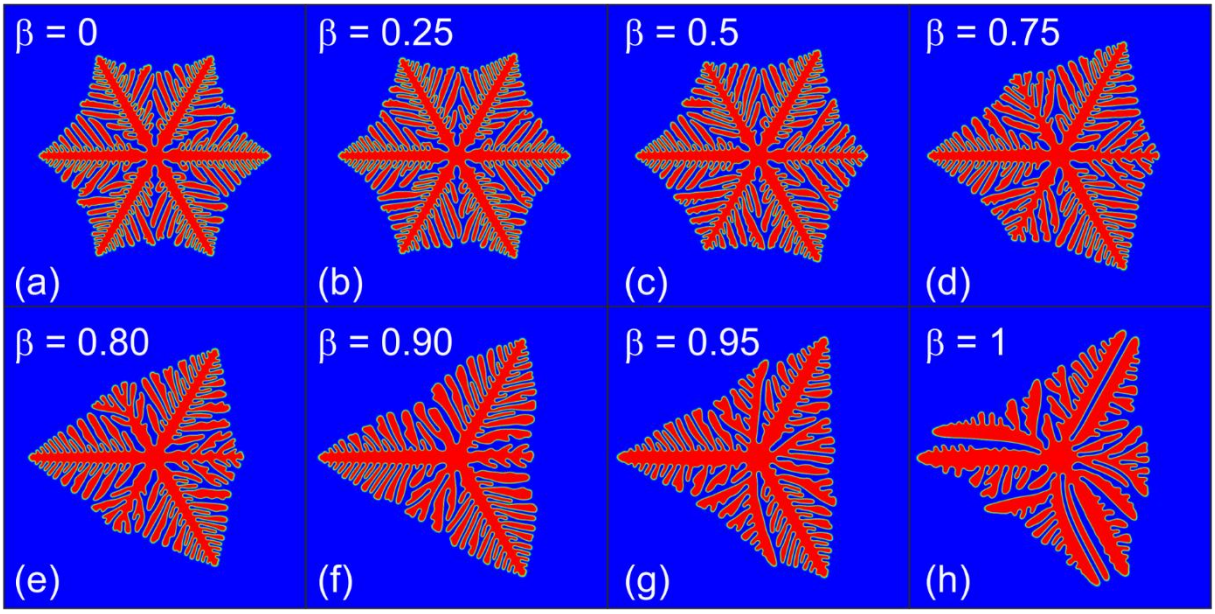


**Figure 3.** (a)-(h) The self-organized structures obtained as a result of phase-field computer simulation with parameters presented in Table 1. Only $\beta$ parameter was changed during the subsequent simulations.

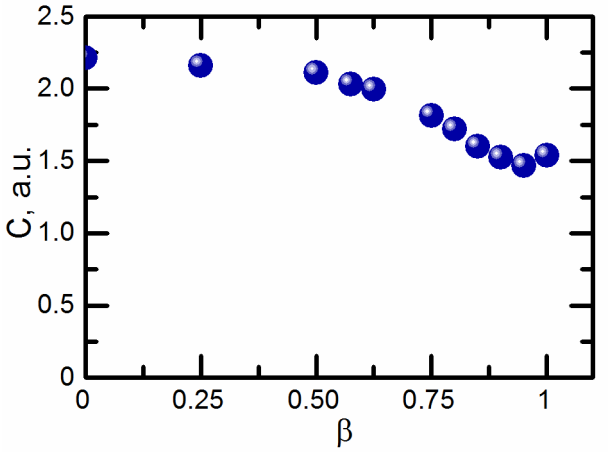


**Figure 4.** The dependence of the envelope shape constant calculated by equation (7) on the relative input of the $C_3$ symmetry term $\beta$.

The envelope shape constant decreases from the value about 2.3 for hexagonal shape to the value about 1.5 for the triangular shape (Fig. 4). The slight increase of the shape constant near $\beta = 1$ can be related to the formation of doublons oriented along $C_3$ symmetry axes (Fig. 3h).

The influence of the noise on the symmetry of obtained structures has been studied. The structures with parameters presented in Table 1 and the pure $C_6$ symmetry ($\beta = 0$, see Figure 3a) and the noise amplitude $a$ from 0 to 0.012 have been analyzed. The symmetry of the structure was estimated according to the following procedure. The binary image of the structure was rotated to the angle 60° with respect to the center of the image. The overlap integral between the initial image and the rotated one was calculated. The overlap integral was normalized to the whole area of the structure. Obtained dependence of normalized overlap integral ($I$) on the noise value is presented in Figure 5. The increase of the noise leads to decrease of the structure symmetry. The relatively high values of the normalized overlap integral for all studied noise amplitudes demonstrates system's stability against noise.

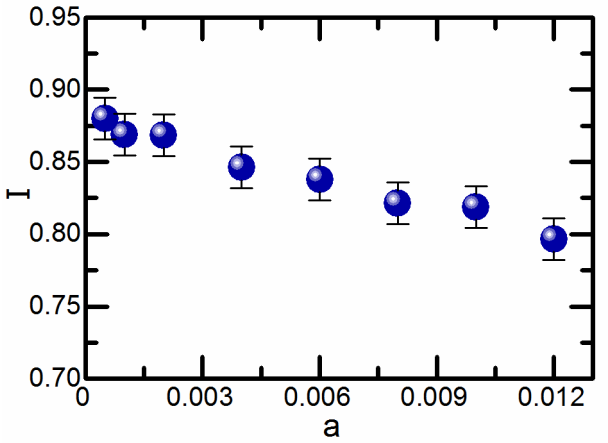


**Figure 5.** The dependence of normalized overlap integral on the noise amplitude.

## 4. Conclusion

The self-organized phase growth with three-fold symmetry has been studied by computer simulation based on the phase-field model. The similarity of simulated and experimentally observed shapes of isolated domains has been achieved. It has been shown that by varying the relation between the $C_3$ and $C_6$ symmetry terms in the interface energy anisotropy formula we can obtain the $C_3$ and $C_6$ envelope symmetries of the obtained structures. It has been shown that the increase of the noise value leads to the decrease of the structure symmetry. However, the relatively high values of the normalized overlap integral for all studied noise amplitudes demonstrate system's stability against noise.

## Acknowledgements

The equipment of the Ural Center for Shared Use "Modern nanotechnology" UrFU was used. The research was made possible by Russian Science Foundation (Project №14-12-00826).

## References

[1] Chen L-Q 2002 Phase-field models for microstructure evolution *Annu. Rev. Mater. Res.* **32** 113-40
[2] Kobayashi R 1993 Modeling and numerical simulations of dendritic crystal growth *Phys. D Nonlinear Phenom.* **63** 410-23
[3] Wheeler A A, Murray B T and Schaefer R 1993 Computation of dendrites using a phase field model *Phys. D Nonlinear Phenom.* **66** 243-62
[4] Shur V Ya, Nikolaeva E V, Shishkin E I, Chernykh A P, Terabe K, Kitamura K, Ito H and Nakamura K 2002 Domain shape in congruent and stoichiometric lithium tantalate *Ferroelectrics* **269** 195-200
[5] Shur V Ya, Chezganov D S, Nebogatikov M S, Baturin I S and Neradovskiy M M 2012 Formation of dendrite domain structures in stoichiometric lithium niobate at elevated temperatures *J. Appl. Phys*. **112** 104113
[6] Shur V Ya and Akhmatkhanov A R 2017 Domain shape instabilities and dendrite domain growth in uniaxial ferroelectrics *Phil.Trans.R. Soc.* A *in press* (doi: 10.1098/rsta.2017.0204)
[7] Shur V Ya, Akhmatkhanov A R and Pelegova E V 2016 Self-organizing formation of dendrite domain structures in lithium niobate and lithium tantalate crystals *Ferroelectrics* **500** 76-89
[8] Shur V Ya, Kosobokov M S, Mingaliev E A, Kuznetsov D K and Zelenovskiy P S 2016 Formation of snowflake domains during fast cooling of lithium tantalate crystals *J. Appl. Phys.* **119** 144101
[9] Brener E 2000 Structure formation in diffusional growth and dewetting *Solid State Ionics* **131** 23-33
[10] Brener E, Müller-Krumbhaar H and Temkin D 1996 Structure formation and the morphology diagram of possible structures in two-dimensional diffusional growth *Phys. Rev.* E **54** 2714-22
[11] Shur V Ya, Gruverman A L and Rumyantsev E L 1990, Dynamics of domain structure in uniaxial ferroelectrics *Ferroelectrics* **111** 123-31
[12] Shur V Ya 1996 Fast polarization reversal process: evolution of ferroelectric domain structure in thin films *Ferroelectric Thin Films: Synthesis and Basic Properties. Ferroelectricity and Related Phenomena, vol. 10* ed C A Paz de Araujo, J F Scott and G W Taylor (Amsterdam: Gordon & Breach Science Publ.) pp 153-192
[13] Shur V Ya 2005 Correlated nucleation and self-organized kinetics of ferroelectric domains *Nucleation Theory and Applications* Ed J W P Schmelzer (WILEY-VCH, Weinheim) pp 178-214
[14] McGilly L J, Yudin P, Feigl L, Tagantsev A K and Setter N 2015 Controlling domain wall motion in ferroelectric thin films *Nat. Nanotechnol.* **10** 145-50
[15] Zelenovskiy P S, Shur V Ya, Kuznetsov D K, Mingaliev E A, Fontana M and Bourson P 2011 Visualization of nanodomains in lithium niobate single crystals by scanning laser confocal

Raman microscopy *Phys. Solid State* **53** 109-13
[16] Soergel E 2005 Visualization of ferroelectric domains in bulk single crystals *Appl. Phys.* B **81** 729-51
[17] Shur V Ya and Zelenovskiy P S 2014 Micro- and nanodomain imaging in uniaxial ferroelectrics: joint application of optical, confocal Raman and piezoelectric force microscopy *J. Appl. Phys.* **116** 066802
[18] Shur V Ya, Akhmatkhanov A R, Chuvakova M A, Dolbilov M A, Zelenovskiy P S and Lobov A I 2017 Formation of self-organized domain structures with charged domain walls in lithium niobate with surface layer modified by proton exchange *J. Appl. Phys.* **121** 104101
[19] Shur V Ya and Rumyantsev E L 1993 Crystal growth and domain structure evolution *Ferroelectrics* **142** 1-7